

# An Early Warning System for Asteroid Impact

JOHN L. TONRY

Institute for Astronomy, University of Hawaii

Received 2010 September 3; accepted 2010 November 2; published 2011 December 15

**ABSTRACT.** Earth is bombarded by meteors, occasionally by one large enough to cause a significant explosion and possible loss of life. It is not possible to detect all hazardous asteroids, and the efforts to detect them years before they strike are only advancing slowly. Similarly, ideas for mitigation of the danger from an impact by moving the asteroid are in their infancy. Although the odds of a deadly asteroid strike in the next century are low, the most likely impact is by a relatively small asteroid, and we suggest that the best mitigation strategy in the near term is simply to move people out of the way. With enough warning, a small asteroid impact should not cause loss of life, and even portable property might be preserved. We describe an early warning system that could provide a week’s notice of most sizeable asteroids or comets on track to hit the Earth. This may be all the mitigation needed or desired for small asteroids, and it can be implemented immediately for relatively low cost. This system, dubbed Asteroid Terrestrial-Impact Last Alert System (ATLAS), comprises two observatories separated by about 100 km that simultaneously scan the visible sky twice a night. Software automatically registers a comparison with the unchanging sky and identifies everything that has moved or changed. Communications between the observatories lock down the orbits of anything approaching the Earth, within one night if its arrival is less than a week. The sensitivity of the system permits detection of 140 m asteroids (100 Mton impact energy) three weeks before impact and 50 m asteroids a week before arrival. An ATLAS alarm, augmented by other observations, should result in a determination of impact location and time that is accurate to a few kilometers and a few seconds. In addition to detecting and warning of approaching asteroids, ATLAS will continuously monitor the changing universe around us: most of the variable stars in our Galaxy, many microlensing events from stellar alignments, luminous stars and novae in nearby galaxies, thousands of supernovae, nearly a million quasars and active galactic nuclei, tens of millions of galaxies, and a billion stars. With two views per day ATLAS will make the variable universe as familiar to us as the sunrise and sunset.

*Online material:* color figures

## 1. INTRODUCTION

In recognition of the hazard posed to the Earth by asteroid impact, Congress has mandated that NASA undertake a Near Earth Object (NEO) survey program to detect, catalog, and track NEOs of 140 m diameter and larger. The recent passage of a 7 m diameter asteroid 2009 VA in 2009 November within only one Earth diameter emphasizes that this is a real threat, and the fact that only a small fraction of such close passages are detected reminds us that we are in fact in a continuous storm of small asteroids passing close by. In the previous year, the Earth was struck by 2008 TC<sub>3</sub> on 2008 October 7 in the Sudan.<sup>1</sup> Perhaps more disturbing, on 2009 October 8, a ~50 kton atmospheric explosion occurred over Indonesia that is thought to have been caused by a ~10 m asteroid impacting the atmosphere.<sup>2</sup>

The article by Asphaug (2009) reviews what is known about asteroid populations and characteristics. (We use the term *asteroid* to mean any small solar system body, asteroid, comet, meteor, etc.) The population of asteroids is quite well known as a function of brightness, usually characterized by the  $H$  magnitude ( $V$ -band magnitude the asteroid would have at 1 AU distance from both the Sun and observer, viewed at opposition). The number of main belt asteroids depends on size as an approximate power law of exponent  $-2.5$ , but the number of small (less than 200 m) NEOs reported by Brown et al. (2002) has an exponent closer to  $-4$ . Since the arrival impact energy scales as the cube of the asteroid size, the net arrival energy is more or less uniform per logarithmic size interval.

Conversion from observed population to surface destruction involves an estimate of albedo to derive size (usually taken as a weighted average of  $\sim 0.14$ , combining  $\sim 0.20$  for the S-type asteroids that predominate among NEOs and  $\sim 0.05$  for the C-type that are the most numerous in the solar system), an estimate of density to derive mass (usually taken as  $\sim 2\text{--}3\text{ g cm}^{-3}$  for S-type, although ice-dominated comets have a density less than

---

<sup>1</sup> A description and references can be found at the JPL NEO website, [neo.jpl.nasa.gov/news/2008tc3.html](http://neo.jpl.nasa.gov/news/2008tc3.html).

<sup>2</sup> The JPL description is at [neo.jpl.nasa.gov/news/news165.html](http://neo.jpl.nasa.gov/news/news165.html).

water, C-type are  $\sim 1.5 \text{ g cm}^{-3}$ , and M-type may have a density in excess of  $6 \text{ g cm}^{-3}$ , an estimate of arrival velocity (typically  $\sim 15 \text{ km s}^{-1}$ , but there is a broad distribution), and an estimate of the fraction of energy that couples through the atmosphere to ground destruction. An asteroid of  $H$  magnitude of 22 is therefore taken to have a diameter of 140 m and to carry about 100 Mton of kinetic energy. Morbidelli et al. (2002) performed this calculation in much more detail and fidelity.

The atmosphere has a surface density equivalent to about 10 m of water, so we can expect that an impactor must be *considerably* larger than  $\sim 10$  m before a substantial fraction of its kinetic energy reaches the ground instead of being dissipated in the atmosphere. For example, Melosh and Collins (2005) calculated that the  $\sim 30$  m iron impactor that created the 1.2 km Meteor Crater in Arizona delivered only  $\sim 2.5$  Mton to the ground of  $\sim 9$  Mton of arrival kinetic energy.

Boslough and Crawford (2008) performed a detailed hydrocode calculation of low-altitude air bursts from asteroid impact, using the Tunguska explosion that flattened trees over an area of  $\sim 1000 \text{ km}^2$  in 1908 as a calibrator, and found that it is not a good assumption to compare an asteroid impact to a stationary point explosion (e.g., nuclear bomb test) at the altitude where the asteroid explodes. One difference is that the wake from the incoming object creates a channel by which the explosion is directed upward, and even a few-megaton explosion will rise hundreds of kilometers into space. Another difference is that the incoming momentum carries the fireball and shock wave much lower than an equivalent point explosion, causing commensurately more damage on the ground. They also performed a calculation of the effects of a 100 Mton stony impactor and found that although the asteroid explodes before it hits the ground, the fireball touches down over a diameter of 10 km with temperatures in excess of 5000 K for 10 s.

The 2007 impact in Carancas, Peru, of a relatively small ( $\sim 3$  m, 1 ton kinetic energy) chondrite left a 13 m crater. This seems to indicate that there are mechanisms by which a small impactor can couple significant energy to the ground, although most, like 2008 TC<sub>3</sub> or the explosion over Indonesia in 2009, will explode harmlessly, high in the atmosphere.

We are therefore left with some uncertainty about the frequency of damage from asteroid impact. The calibration by Brown et al. (2002) of small NEOs is based on the rate of large fireballs from atmospheric impacts and a conversion from optical to explosion energy, and this is joined onto estimates from counts of asteroids as a function of  $H$  magnitude. The rate of impacts by large asteroids (140 m and larger) is estimated to only one per 20,000 yr or more, the rate of impacts by 50 m Tunguska-sized objects (5 Mton arrival kinetic energy) is about one per 1000 yr, and the rate of 10 m (40 kton arrival kinetic energy) impacts is about one per decade (NRC 2010). These rates are probably uncertain to a factor of at least two, and the work of Boslough and Crawford (2008) illustrates the dif-

ficulty in predicting surface damage from the incident kinetic energy.

A NASA NEO report (2007) found that a combination of planned surveys by Pan-STARRS 4 (Panoramic Survey Telescope and Rapid Response System, PS4) and LSST (Large Synoptic Survey Telescope) could reach 83% completeness for 140 m diameter NEOs by 2026. The total architecture cost was estimated at about \$500 million in fiscal year 2006 dollars. In order to speed up and improve the detection probability, NASA found that an additional \$800 million to \$1 billion for either an additional LSST system dedicated to potentially hazardous object (PHO) detection or a dedicated space imager could bring the completion limit to better than 90% by 2020.

This conclusion was affirmed in the recent report by the NRC (2010) on survey and mitigation strategies that NASA might pursue to reduce the risk from hazardous objects, but they stressed the severe tension between cost and survey completion deadline and suggested that 2030 may be a more attainable goal, although still at high cost. The NRC report (2010) also recognized that the damage from relatively small asteroids in the 30–50 m range may be greater than heretofore appreciated, and it recommended that “surveys should attempt to detect as many 30–50-meter objects as possible.”

We believe that, while the final solution of finding, cataloging, and tracking 90% of asteroids of 140 m is very hard, the technology to find most asteroids of 50 m or larger on their final approach is now in hand. Although this may not give us enough warning to mount a mission to deflect the asteroid, it should give us enough warning to know exactly where and when the impact will occur. Lives can be saved by moving out of the impact area or away from the tsunami run-up, even though loss of property is unavoidable.

We describe how the construction and operation of a new sky survey could continually scan the visible sky. This facility, entitled Asteroid Terrestrial-Impact Last Alert System (ATLAS) would use an array of eight wide-field, fast telescopes equipped with large detector arrays to scan the visible sky ( $\sim 20,000 \text{ deg}^2$ ) twice per night. Its sky completeness gives us a better than 50% chance of detecting any 50 m asteroid approaching from a random direction, and its sensitivity provides three weeks’ warning of 140 m objects and one week for 50 m asteroids.

The second section discusses the general meaning of etendue and presents equations for survey capability and signal-to-noise ratio (S/N) achievable from a survey instrument, even in the regime of undersampled pixels. This lays the foundation for evaluation of how scientific goals can be met by a given survey implementation. The third section presents details of the ATLAS concept and describes how it compares with other surveys, present and planned. The fourth section describes how ATLAS performs in its role of detecting hazardous asteroids as well as other science topics. We find that ATLAS has some very interesting capabilities beyond early warning and is quite complementary to other existing or planned surveys. We conclude with

thoughts on how ATLAS could provide the seed for a World-wide Internet Survey Telescope that could improve the probability of detection and the warning time of approaching impactors.

## 2. ETENDUE AND SURVEY DESIGN

### 2.1. Etendue and Information

The technical term *etendue* means the product in an optical system of the solid angle and cross-sectional area occupied by the bundle of light rays. Liouville’s theorem guarantees that this product is conserved throughout the optical system, provided there is no absorption. In particular, at the entrance aperture, the product of solid angle seen on the sky times the collection area is a measure of how large the “grasp” of an optical system is. This etendue product is therefore often adopted as a measure of the merit of proposed survey systems, with some understanding that it has something to do with the rate at which scientific value can be accrued.

The information content in  $N$  independent measurements at S/N  $S$  is expressible in  $N \log_2(S)$  bits. If our science goal is to generate a catalog of independent quantities, this might be an appropriate metric for the tradeoff between quantity  $N$  against quality  $S$  to maximize information. However, an important and common science goal is accumulation of S/N for a measurement to which many correlated observations contribute. In this case the science value lies in the S/N of the sum or other combination of measurements that are presumed to be highly correlated, and the information content goes as  $\log_2(N^{1/2}S)$ , or  $\sum \frac{1}{2} \log_2(n_i S_i^2)$  if we do this for a number of classes of inquiry, collecting  $n_i$  objects in each class with S/N  $S_i$ . Colloquially, the net S/N from averaging  $N$  measurements improves as  $N^{1/2}$ .

This sum,  $\log(n_i S_i^2)$ , is in fact the standard metric that is used to evaluate the capability of a survey system. It is not unique, nor is it appropriate for all scientific goals (for example, it does not optimize detection rate of stellar occultations by hot Jupiters, where the dependency of capability on  $S_i$  is essentially a step function at  $S_i \sim 200$ ), but it does describe the main scientific purposes to which survey data are usually applied. We will use the term *capability* henceforth to mean “accumulation of  $\log(n_i S_i^2)$  per unit time” in order that etendue can be reserved for its technical use.

In the Poisson limited case, where the variance is proportional to the number of photons collected and  $n_i$  is proportional to the solid angle surveyed,  $n_i S_i^2$  does not depend on how survey time is apportioned between area coverage and depth—capability is basically the number of photons collected from objects of class  $i$ , regardless from which objects the photons come. There are two curbs on this covariance, apart from the details of luminosity function or spatial distribution. The first arises when systematic error at extremely low or high  $S_i$  (e.g., read noise or flatfielding error) slows the growth of information from  $n_i^{1/2}$ —it is often not practical to increase  $n_i$  without bound by permitting  $S_i$  to become arbitrarily small, nor do we

necessarily gain by arbitrarily increasing  $S_i$  on a single object. The second limit arises when  $n_i$  becomes so large within a solid angle that objects blur together—their perceived fluxes are no longer independent, which again limits the growth of information. If we assign a footprint solid angle  $\omega$  to an object blurred by the point-spread function (PSF) and consider an object to have value only if no other object’s footprint overlaps its center, the maximum density of isolated objects is achieved when the overall number density is  $\omega^{-1}$ , at which point the density of non-overlapped objects is lower by the natural logarithm base,  $(e\omega)^{-1}$ .

Apart from these considerations, and for known objects with sufficient density on the sky or randomly positioned objects, maximizing  $n_i$  is tantamount to maximizing the solid angle that can be observed per unit time. Therefore, we can consider the survey metric to be  $\Omega S_i^2$ , where  $\Omega$  is the survey solid angle, but remembering that this is not valid when  $S_i$  is low enough to be affected by systematics or when the PSF and object footprint are large enough that objects start to overlap. The survey capability is the rate at which  $\Omega S_i^2$  is accumulated.

### 2.2. S/N and PSFs

Recovery of an unresolved object’s flux in the face of blurring and noise is a finely honed art. For uniform, independent Gaussian noise the optimum S/N occurs by cross-correlating (often misnamed convolving) the image with the PSF. More generally, the optimum cross-correlation kernel is just the Wiener filter, whose Fourier transform depends on those of the PSF,  $P(k)$ , and the noise,  $N(k)$ :  $|P|^2/(|P|^2 + |N|^2)$ . In the limit that an object is faint compared with the noise, the optimum kernel then devolves to the PSF itself, but if the object’s noise variance is significant or if the background noise is correlated (e.g., by rebinning), the optimal kernel becomes narrower in image space.

Note that this is true for undersampled images as well, where it is understood that the kernel is the convolution of a physical PSF (meaning distribution of delivered flux prior to integration within a pixel) with a detector pixel *with phase shift*; i.e., the optimal kernel depends on the exact subpixel position where the object lies.

The net S/N from a faint point source of total flux  $f$  spread over a unity integral PSF  $P$ , in the face of independent Gaussian noise variance per unit area (square arcseconds, for example)  $\sigma^2$ , derived from integration against a unity integral kernel  $K$  is just

$$S/N = \frac{f}{\sigma} \frac{\int KP}{[\int K^2]^{1/2}} = \frac{f}{\sigma} [\int P^2]^{1/2}, \quad (1)$$

where the right side expresses the S/N when the PSF is used as an optimal kernel.

We integrated equation (1) for a variety of popular PSF models, with results from the well-sampled regime given in Table 1.

TABLE 1  
 S/N FOR DIFFERENT PSFS

PSF (1)	$\alpha_{\text{PSF}}$ (2)	$\alpha_{\text{circ}}$ (3)	$r_{\text{circ}}$ (4)	Atm? (5)
Gaussian .....	0.66	0.60	0.70	N
Kolmogorov .....	0.57	0.51	0.71	Y
Moffat .....	0.58	0.51	0.73	Y
Waussian .....	0.52	0.45	0.76	Y
Cubic Lorentzian .....	0.40	0.28	0.84	N

NOTES.—The profiles are Gaussian, a Kolmogorov  $\exp(-k^{5/3})$  profile, a Moffat (power of a Lorentzian) profile  $(1+r^2)^{-\beta}$  with  $\beta = -4.765$  recommended by Trujillo et al. (2001), a “Waussian” (wingy Gaussian)  $(1+r^2+r^4/2+r^6/12)^{-1}$  introduced by Schechter et al. (1993) for DoPhot, and a cubic Lorentzian (i.e., Moffat function with  $\beta = 3/2$ ). Col. (2): proportionality factor  $[(S/N)\sigma(d/f)]$  for a PSF kernel; Col. (3): factor for an optimal circular, top-hat kernel; Col. (4): optimal top-hat radius in units of  $d$ ; Col. (5): PSF profiles that are realistic approximations to atmospheric PSFs.

Since  $[\int P^2]^{1/2}$  for a given PSF must be inversely proportional to the spatial scale in order to maintain unity integral, the S/N will be proportional to  $f/\sigma d$ , where we use the full width at half-maximum (FWHM)  $d$  as a convenient measure of the PSF extent. We see that aperture photometry delivers an S/N that is about 12% worse than PSF integration.

We also performed these integrations into the extremely undersampled regime, averaging  $(S/N)^2$  over PSF position within a square pixel, and found that a reasonable fit to the results for the middle three (atmospheric) PSFs from Table 1 is

$$S/N = \frac{f}{\sigma} (3.5d^2 + 0.4dp + p^2)^{-1/2}, \quad (2)$$

where  $d$  is the *physical* FWHM,  $p$  is the pixel size,  $\sigma^2$  is the background noise variance per unit area, and  $f$  is the total flux in the faint point source. Equation (2) is therefore a good approximation for atmospheric PSFs, regardless of undersampling.

An application of equation (2) is selection of pixel size for optimal S/N, trading off read noise against background noise variance. (For zero read noise the optimum is an infinitely small pixel.) If we add  $\sigma_R^2/p^2$  to  $\sigma^2$ , where  $\sigma_R$  is the read noise per pixel, we can solve for the pixel size that maximizes the S/N. An approximate solution to the quartic equation is given by

$$p_{\text{opt}}^2 = 2d\sigma_R/\sigma. \quad (3)$$

Since  $\sigma_R/\sigma$  is the pixel size at which the read noise equals the sky noise, the pixel that optimizes photometry S/N is  $\sqrt{2}$  times the geometric mean of the physical FWHM and the size that balances read noise against sky noise (which depends on bandpass and sky brightness).

### 2.3. Survey Design and Performance

A survey system’s ability to capture photons from a source depends on its aperture and obstruction, vignetting, filter bandwidth and throughput, atmospheric throughput, detector quantum efficiency, and fill factor, which we bundle into a single throughput number  $\epsilon$ . Operationally, we use the zero point of the AB magnitude system,  $5.48 \times 10^6$  photons  $\text{cm}^{-2} \text{s}^{-1} \ln(\nu_2/\nu_1)^{-1}$ , to find that an AB magnitude of  $m_0 = 25.10$  provides 1 photon  $\text{m}^{-2} \text{s}^{-1}$  per bandpass of 0.2 in natural log of wavelength (a typical width for astronomical filters). We define  $\epsilon$  as the factor by which an actual system falls short of this ideal (or conceivably exceeds it by using a broader bandpass); i.e., the signal from a source of magnitude  $m$  captured by an aperture of area  $A$  is

$$f = A\epsilon t_{\text{exp}} 10^{-0.4(m-m_0)}. \quad (4)$$

We define the net fraction of shutter open time, including losses for weather, daytime, instrumental failures, etc., as the *duty cycle*,  $\delta$ . A survey system’s temporal efficiency depends on the net exposure time devoted to a given field,  $t_{\text{exp}}$ , adding together however many successive dithers are deemed necessary, and the matching overhead time  $t_{\text{OH}}$  that adds all proportionate times such as read out, slew, focus, etc. We term the ratio  $t_{\text{exp}}/(t_{\text{exp}} + t_{\text{OH}})$  as the *temporal duty cycle*  $\delta_t$ . The duty cycle  $\delta$  can have an interesting relation to  $\delta_t$ , especially when one considers sites in Antarctica ( $\delta = \delta_t$  in the winter) or in orbit or an observatory that consists of many units at a diversity of geographical locations, but generally speaking, we have control over  $\delta$  when designing a survey but control over only  $\delta_t$  when operating a survey (by changing  $t_{\text{exp}}$ ).

Let us define the PSF footprint  $\omega$  as the solid angle that carries background noise equal to  $f/(S/N)$  for a faint point source of flux  $f$  and S/N defined by the flux measurement algorithm in use (e.g., those in Table 1), so that we can calculate S/N for a given object by comparing its total flux to the noise found in this PSF footprint. Equation (2) gives this solid angle as  $\omega = (3.5d^2 + 0.4dp + p^2)$  for the case of PSF-matched photometry with a atmospheric seeing profile and independent noise, but which is not necessarily well sampled.

If  $\mu$  is the sky brightness per square arcsecond, the noise variance that the signal contends with is

$$\sigma^2 = A\epsilon t_{\text{exp}} (\omega 10^{-0.4(\mu-m_0)} + 10^{-0.4(m-m_0)}) + f_R^2, \quad (5)$$

where  $f_R^2$  is the readout variance over  $\omega$ ’s worth of pixels:  $f_R^2 = \sigma_R^2 p^{-2} \omega$  for a read noise of  $\sigma_R e^-$  and pixel size  $p$  arcseconds.<sup>3</sup>

<sup>3</sup> Note that the term involving the object’s magnitude  $m$  itself is somewhat notional—not only does the weighting involve  $\int P^3$  for the case of a PSF kernel, but the optimal kernel would change for objects that are brighter than noise. Its presence serves to remind us that S/N depends on the Poisson statistics of the flux from the object itself.

Equations (4) and (5) provide the square of the S/N,  $S_1^2$ , for at this particular magnitude:

$$S_1^2 = A\epsilon t_{\text{exp}} \omega^{-1} 10^{+0.4(\mu-m_0)} 10^{-0.8(m-m_0)} \times [1 + 10^{-0.4(m-m_{\text{sky}})} + f_R^2 f_{\text{sky}}^{-1}]^{-1}, \quad (6)$$

where  $m_{\text{sky}}$  is sky magnitude within  $\omega$ ,  $m_{\text{sky}} = \mu - 2.5 \log \omega$ , and  $f_{\text{sky}}$  is equivalent flux in  $e^-$ ,  $f_{\text{sky}} = A\epsilon t_{\text{exp}} 10^{-0.4(m_{\text{sky}}-m_0)}$ . In this equation and subsequently, the term in square brackets is approximately unity when the sky noise dominates the object's photon statistics and the read noise; we include it here for completeness, but drop it henceforth for clarity. It can be reintroduced if the read noise or object photon noise is significant with respect to the background noise.

The capability metric defined previously includes a factor for the surveyed solid angle. The cadence time  $t_{\text{cad}}$  to carry out  $t_{\text{exp}}$  worth of integration over a survey solid angle  $\Omega$  is related to the field-of-view solid angle  $\Omega_0$  and duty cycle by

$$\Omega t_{\text{cad}}^{-1} = \Omega_0 t_{\text{exp}}^{-1} \delta. \quad (7)$$

Therefore, the capability function at magnitude  $m$  is

$$\frac{S_1^2 \Omega}{t_{\text{cad}}} = \frac{A \Omega_0 \epsilon \delta}{\omega} 10^{+0.4(\mu-m_0)} 10^{-0.8(m-m_0)}. \quad (8)$$

This includes the  $A \Omega_0$  term commonly called *etendue*, but also the dependence on  $\omega$ ,  $\epsilon$ ,  $\delta$ , and  $\mu$  that are crucial to the real S/N gathering capability of a system. Rewriting the system-fixed parameters as an overall system capability  $M$ , equation (9) reveals how the survey choices of cadence, S/N, survey area, and magnitude can be traded off against one another:

$$M = \frac{A \Omega_0 \epsilon \delta}{\omega} 10^{+0.4(\mu+m_0)} = \frac{S_1^2 \Omega}{t_{\text{cad}}} 10^{+0.8 m}. \quad (9)$$

Taking a logarithm, survey-variable parameters on the right add to the (nearly) constant left-hand side:

$$\log M = 0.8 m - \log t_{\text{cad}} + \log \Omega + 2 \log S_1. \quad (10)$$

This relation forms a surface in the observability space of magnitude  $m$ , S/N, solid angle, and cadence interval that is accessible for a particular survey capability. The left-hand side is not strictly fixed; changing  $t_{\text{exp}}$  affects  $\delta_t$  and  $\delta$ , as well as the (dropped) term in square brackets if the read noise is not negligible, and the term in square brackets also contributes if the object is brighter than the background. A sketch of how the left-hand side is affected is illustrated in Figure 1. Apart from this, the observability surface is a plane in log space.

As argued in the preceding section, most science value is not changed by tradeoffs that keep the product  $\Omega S_1^2$  constant. In

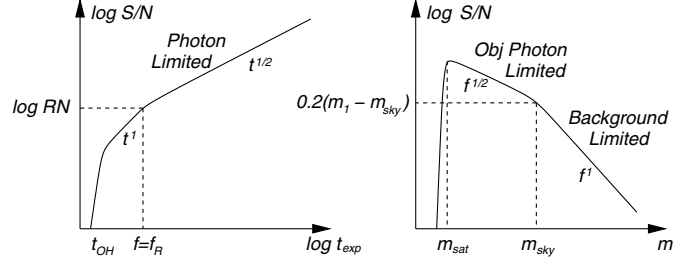


FIG. 1.—S/N, illustrated by cuts at constant magnitude and  $t_{\text{exp}}$ , falls precipitously when  $t_{\text{exp}}$  approaches the overhead time  $t_{\text{OH}} (\delta_t \ll 1)$  or the magnitude approaches the saturation limit  $m_{\text{sat}}$  (which depends on  $t_{\text{exp}}$  of course), falls quickly with exposure time when the flux is less than the read noise  $f_R$ , and transitions between photon and background limited when the magnitude becomes fainter than the background magnitude  $m_{\text{sky}}$  within a PSF.

practice, scientists tend to set  $S_1$  at a fixed minimum value for which systematics are not compromising the S/N and then maximize survey solid angle  $\Omega$ . For moving-object detection,  $S_1$  might be 5; for Type Ia supernova light curves,  $S_1$  might be 30 at peak; and for planetary occultations,  $S_1$  might be 200. This science value level set or S/N operating point provides a second constraint in observability space for a survey. Therefore, there are really only two independent parameters for setting a given survey's operation for a given capability: for a given magnitude the cadence time dictates the solid angle.

The density of various types of objects and application of science values can now optimize the overall survey capability. For example, if value lies in detection of orphan afterglows of gamma-ray bursts (GRBs), we may choose to spend our  $M$  capability in short  $t_{\text{cad}}$  and large  $\Omega$  at the expense of  $m$ . If value lies in detection of planetary occultations of stars, we cannot give up  $S_1$  or  $t_{\text{cad}}$  and therefore may make compromises in  $m$  or  $\Omega$ . Searching for solar system objects would emphasize  $m$  and  $\Omega$  at the cost of minimal  $S_1$  and allowing  $t_{\text{cad}}$  to grow to the linking confusion limit. General-purpose surveys such as PTF (Palomar Transient Factory), Pan-STARRS, and SkyMapper strive to maximize capability  $M$  generally, but then dedicate portions of time (subdivide  $\delta$ ) to different locations in the observability surface according to different science goals. LSST has claimed to be able to maximize science value at a fixed location on the observability surface, but, of course, it is straightforward to move on the surface or split time into different surveys, should that prove desirable.

### 3. ATLAS

Spaceguard has discovered most NEOs larger than 1 km and has determined that none will strike the Earth in the foreseeable future. The NRC report (2010) estimates that the remaining fatality rate is bimodal as a function of impactor size, with a  $10^{-6} \text{ yr}^{-1}$  probability of impact by a 1–2 km object that would cause 50 million deaths (averaging over possible impact locations) and a  $10^{-3} \text{ yr}^{-1}$  probability of impact by a ~50 m object

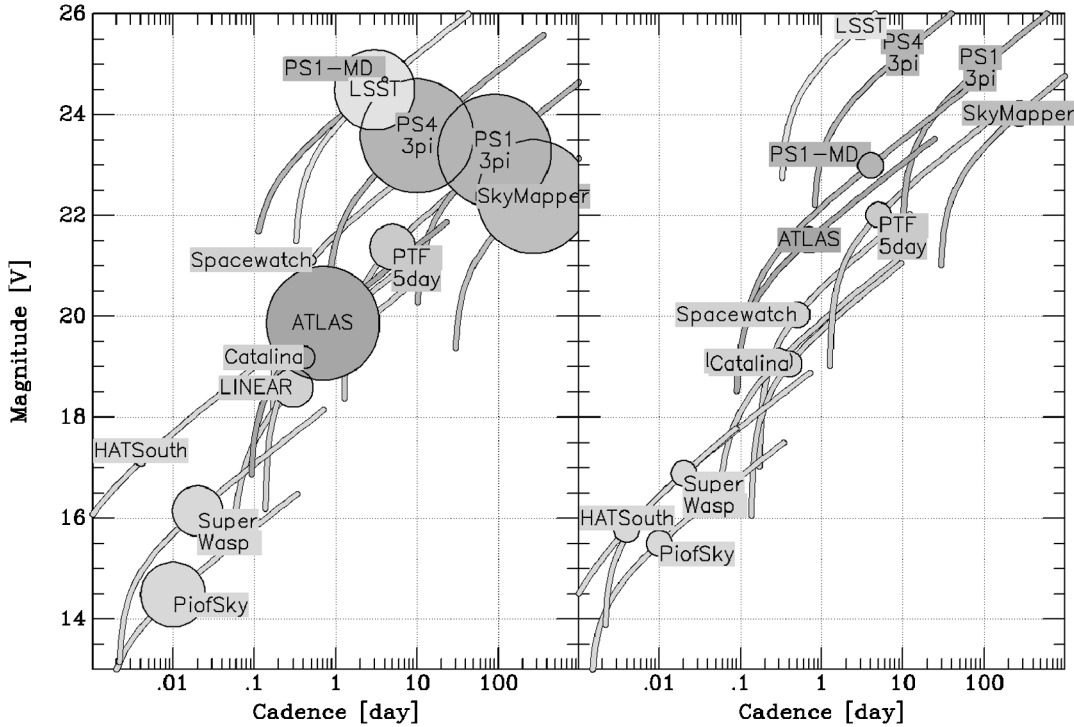


FIG. 2.—*Left*: Various systems’ capabilities at common  $S/N = 5$  in the magnitude-cadence plane. The area of the symbol is proportional to the solid angle  $\Omega$  surveyed in that cadence time, and the lines illustrate the observability surface in  $m$  and  $t_{\text{cad}}$  at fixed  $\Omega$  and  $S/N$ . However, putting all surveys at a common  $S/N = 5$  does some injustice to the science they seek to achieve. The rolloff in magnitude occurs when  $t_{\text{exp}}$  becomes comparable with  $t_{\text{OH}}$  (the square bracket term). *Right*: Various systems capabilities in the magnitude-cadence plane at common  $S/N = 5$  and assuming they trade off sensitivity for coverage to  $\Omega = 1000 \text{ deg}^2$ . See the online edition of the *PASP* for color version of this figure.

that would cause an average of 30,000 deaths. The  $H$  magnitude of a 50 m asteroid is 24 or fainter, and for a typical phase function the actual magnitude at 1 AU distance will be greater than 25–26. This suggested to us that surveying at a much smaller distance than 1 AU would make sense and, by definition, any Earth-impacting asteroid will be present shortly before impact at a small distance. Choosing one week as a minimum warning interval for civil defense against a limited explosion and three weeks’ warning as necessary for a city-devastating explosion, we were surprised to discover that this places rather modest requirements on limiting magnitude, although it does require isotropic vigilance.

It is possible to achieve the requisite sensitivity over half of the sky with survey hardware that is more or less off-the-shelf and of modest cost. We have proposed ATLAS to NASA for construction and 2 yr of operation; fundamentally, the system is equivalent to a telescope of 0.5 m aperture with a  $40 \text{ deg}^2$  field of view, subjected to an effective PSF of  $3.8''$ , with bandpasses twice as wide as an SDSS filter. By comparison, the PTF uses a 1.2 m aperture, an  $8 \text{ deg}^2$  field of view, and SDSS filters and enjoys  $\sim 2.2''$  seeing for a very comparable capability.

The NASA proposal implements ATLAS using eight Takahashi astrographs of 0.25 m aperture and 0.7 m focal length

that each provide a  $20 \text{ deg}^2$  field of view. These telescopes are small enough that there are a number of equatorial mounts available commercially that can carry more than one telescope. We believe that a fully equipped telescope with focuser, filters, shutter, camera adapter, and mount should cost about \$50,000.

The cameras for ATLAS each have a  $4000 \times 4000$  pixel focal plane, taking advantage of an existing inventory of  $2000 \times 4000$  CCDs with 15  $\mu\text{m}$  pixels. Although the pixel size is not optimal in the preceding sense (a 10  $\mu\text{m}$  pixel provides about 0.1 mag more sensitivity in moderate seeing), a pair of those CCDs could be mounted in a cryostat and equipped with a controller for a unit cost that we again believe will be about \$50,000 (since there is no detector cost).

ATLAS consists of a set of eight of these telescope and camera units and reaches an interesting survey capability level, while remaining cost-effective. While subject to further optimization, the design reference calls for the following:

1. Exposures of  $t_{\text{exp}} = 30 \text{ s}$  with  $t_{\text{OH}} = 5 \text{ s}$  and  $10 e^-$  read noise, using broad filters that are approximately  $g + r$  and  $r + i$ . (The science program of finding asteroids calls for the broadest possible filters; the other science programs benefit from color information.)

2. Four unit telescopes are clustered on a common mount within an observatory, and the other four are in an identical observatory separated by  $\sim 100$  km in order to obtain good parallaxes to 0.1 AU, enabling instantaneous alerts for approaching objects, as well as providing the crucial function of weeding out false alerts from space junk. The blue observatory uses the  $g + r$  filter set; the red observatory uses the  $r + i$  filters. At each observatory telescopes are used as two co-aligned pairs, thereby providing  $40 \text{ deg}^2$  of instantaneous field of view at twice the aperture of a single telescope and twice the throughput of a single SDSS filter. The two observatories synchronize their pointing and observations exactly.

3. Both observatories cover the entire visible sky ( $20,000 \text{ deg}^2$ ) twice per night, visiting each point with a time separation of about 1 hr (R.A. permitting) in order to obtain unambiguous tracklets of moving objects.

Although the 15  $\mu\text{m}$  pixels subtend  $4.4''$  and are therefore considerably undersampling the PSF, a detailed calculation of the expected sensitivity is promising. A single moonless exposure in either bandpass by each of the telescopes reaches  $S/N = 5$  at  $V = 19.1$  for a solar spectrum. The seeing assumed for this was  $1.5''$ , but the  $S/N$  is relatively insensitive because of the undersampling, and the contribution from optics blur. The sum of the images from a co-aligned pair of units therefore yields  $S/N = 5$  at  $V = 19.5$ . The combination of the observations from the two co-aligned pairs at the two observatories provides  $S/N = 5$  at  $V = 19.9$ . (The two filters are chosen to provide the same  $S/N$  for a solar spectrum.)

ATLAS's performance on objects fainter than this depends on the details of the object and how the observatories can communicate. Our design calls for each observatory to have a cluster of computers that can align and co-add images and that can reliably detect objects at  $S/N = 3.7$  (with false alarms). We demand that the observatories have at least enough bandwidth that they can share detections, so as to confirm  $S/N = 3.7$  detections and reach  $S/N = 5$  at  $V = 19.9$ .

We cannot expect to detect moving objects (or objects closer than 0.05 AU with a significant parallax) much fainter than  $V \sim 20$ , since they will not align on successive images. However, stationary objects that are observed twice per night will be detected at  $S/N = 5$  at  $V \sim 20$  in both the red and blue bandpasses or at  $S/N = 5$  at  $m = 20.35$  in a combination of red and blue images. Obviously detections of stationary objects can continue to fainter magnitudes by stacking many nights' observations until systematics dominate. With no defocus, the cameras will saturate at  $V \sim 12.5$  (blue) and  $V \sim 13$  (red). We intend to equip each observatory with a pair of high-end digital single-lens reflex cameras to provide five-color photometry to a limiting magnitude of  $V \sim 6$ , so as to be able to monitor brighter stars and extend the dynamic range for very bright transients.

#### 4. ONGOING AND PLANNED SURVEYS

There are many past, ongoing, and future sky surveys for a variety of purposes. Table 2 shows the basic design choices made by a set of successful efforts and some proposed ones.

The most productive asteroid and NEO search programs are currently the Catalina Sky Survey<sup>4</sup> (Larson et al. 2003), Lincoln Near Earth Asteroid Research (LINEAR<sup>5</sup>; Stokes et al. 2000), and Spacewatch<sup>6</sup> (McMillan et al. 2006; Larson et al. 2007). The JPL World Wide Web site<sup>7</sup> attributes 73% of asteroid discoveries in 2009 to Catalina (60% of NEOs), 14% to LINEAR (28% of NEOs), and 8% to Spacewatch (4% of NEOs). (Spacewatch is now spending a greater fraction of time on follow-up rather than discovery.)

Pi of the Sky<sup>8</sup> (Malek et al. 2009) is a representative GRB search program. Rapid Telescopes for Optical Response (RAPTOR;<sup>9</sup> Vestrand et al. 2003) is another interesting example of GRB and other transient search, but is not listed in Table 2. These projects put a high premium on rapid cadence and rapid follow-up capability, at the cost of limiting magnitude.

SuperWASP<sup>10</sup> (Wide Angle Search for Planets; Pollacco et al. 2006) and HAT-South<sup>11</sup> (Hungarian-made Automated Telescope; Bakos et al. 2009) are examples of surveys searching for planetary occultations. Such surveys must work at very high  $S/N$  at fast cadence, again at the expense of limiting magnitude, but their science does not lack for stars of suitable brightness. HAT-South is particularly interesting for comparison with ATLAS because there are marked similarities in the equipment, but the science for HAT-South and ATLAS lives in different locations in observability surface.

The PTF<sup>12</sup> (Law et al. 2009) has dedicated time to different search strategies for optical transients such as supernovae. We list the properties of the 5 day portion of their survey.

Pan-STARRS 1<sup>13</sup> (Burgett & Kaiser 2009) and SkyMapper<sup>14</sup> (Keller et al. 2007) seek to perform surveys of the entire northern and southern skies to unprecedented depths. Both surveys are optimized to find transients and moving objects. A portion of Pan-STARRS 1 (PS1) is dedicated to a  $3\pi$  survey of three-fourths of the sky, revisiting once every 3 months; another portion to a medium-deep (MD) survey of about  $40 \text{ deg}^2$  revisited each day to a substantial depth. We list both Pan-STARRS surveys in order to illustrate how more or less equal resources (capability) can be placed at rather different places on the

<sup>4</sup> See <http://www.lpl.arizona.edu/css>.

<sup>5</sup> See <http://www.ll.mit.edu/LINEAR>.

<sup>6</sup> See <http://spacewatch.lpl.arizona.edu>.

<sup>7</sup> See <http://neo.jpl.nasa.gov>.

<sup>8</sup> See <http://grb.fuw.edu.pl>.

<sup>9</sup> See <http://www.raptor.lanl.gov>.

<sup>10</sup> See <http://www.superwasp.org>.

<sup>11</sup> See <http://www.cfa.harvard.edu/~gbakos/HS>.

<sup>12</sup> See <http://www.astro.caltech.edu/ptf>.

<sup>13</sup> See <http://pan-starrs.ifa.hawaii.edu>.

<sup>14</sup> See <http://rsaa.anu.edu.au/skymapper>

TABLE 2  
SKY SURVEY DESIGN AND PERFORMANCE

Program	$A$	$\Omega_0$	$\omega$	$m_{\text{sky}}$	$\delta_t$	$S_1$	$m$	$n_c$	$t_{\text{cad}}$	$\Omega$	$\log M$
NEOSearch											
Spacewatch .....	0.51	2.9	16	18.0	0.50	3	21.7	1	0.5	150	20.8
LINEAR .....	1.2	2.0	30	17.3	0.80	4	19.0	1	0.3	2400	20.4
Catalina .....	0.27	8.2	41	17.0	0.50	4	19.5	1	0.4	800	20.1
GRB Counterparts											
PioftheSky .....	0.13	484	25000	10.0	0.83	5	14.5	1	0.01	6400	18.8
Planet Occultations											
SuperWASP .....	0.15	61	11000	10.9	0.88	100	12.9	1	0.02	3900	19.7
HAT-South .....	0.46	16	128	15.7	0.92	100	14.0	1	0.004	128	20.5
Sky Survey and Transients											
PTF-5day .....	0.85	7.8	16	18.0	0.67	5	21.4	2	5	3200	21.3
SkyMapper .....	1.1	5.2	8	18.7	0.88	5	22.4	6	270	20000	21.2
PS1-3 $\pi$ .....	1.8	7.5	3.7	19.6	0.75	5	23.3	5	90	20000	22.4
PS1-MD .....	1.8	7.5	3.7	19.6	0.98	5	24.7	5	4	45	22.2
Proposed Surveys											
ATLAS .....	0.29	20	46	16.9	0.86	5	19.9	2	0.7	20000	21.8
PS4-3 $\pi$ .....	7.1	7.5	3.0	19.8	0.92	5	23.6	5	10	20000	23.6
LSST .....	35	9.6	2.9	19.8	0.88	5	24.5	2	3	10000	24.5

NOTES.— $A$  is the net aperture in  $\text{m}^2$ , including obscurations and the number of units;  $\Omega_0$  is the solid angle in  $\text{deg}^2$  per exposure;  $\omega$  is the noise equivalent PSF area in square arcseconds, as discussed in the text;  $m_{\text{sky}}$  is the magnitude collected within  $\omega$  when the sky brightness is  $\mu = 21$  per square arcsecond;  $\delta_t$  is the exposure duty cycle  $t_{\text{exp}}/(t_{\text{exp}} + t_{\text{OH}})$ ;  $S_1$  is the S/N achieved at magnitude  $m$ , which includes the coadded sensitivity from the contributions of  $n_c$  colors; the cadence times  $t_{\text{cad}}$  in days have been adjusted for two-thirds clear weather;  $\Omega$  is the actual solid angle in  $\text{deg}^2$  surveyed in the cadence time  $t_{\text{cad}}$ ; Catalina is only the 0.7 m Schmidt, its combination with the Siding Spring Survey and the Mount Lemmon Survey almost double the total capability; PS4-3 $\pi$  presumes a 100% 3 $\pi$  survey for PS4, but the etendue may be split as with PS1; LSST is based on current suggestions for a two-color, 2 $\pi$  survey that is estimated to reach  $m = 24.5$  in 3 days, including weather.

observability surface. Pan-STARRS is intended to be a replicable system, with a goal of four units (PS4) sited on Mauna Kea.

The LSST<sup>15</sup> (Ivezic et al. 2008) is proposed to survey the visible sky on a few-day cadence with an 8 m telescope, projected to reach at least a magnitude fainter than Pan-STARRS 1 at a much faster cadence.

Table 2 also shows how well these surveys perform and their log capability, generated from equation (9). Actual performance only correlates loosely with  $A\Omega_0$ : background, efficiency, and duty cycle are very serious factors. Therefore, the capability is best calculated from the *right*-hand side, since limiting magnitude at some estimate of S/N and the overall cadence of covering a planned solid angle is generally well reported. For systems that are not yet operational we take their estimated S/N and magnitude at face value, but delivered  $\epsilon$ ,  $\delta$ , and, especially,  $\omega$  may fall short of preoperational claims.

Different survey choices can trade off  $m$ ,  $S_1$ ,  $t_{\text{cad}}$ , and  $\Omega$  against one another on the observability surface; Figure 2 shows a cut at constant  $S_1 = 5$  in the  $m - t_{\text{cad}}$  plane, with point area proportional to  $\Omega$  and another cut at  $S_1 = 5$  and  $\Omega = 1000 \text{ deg}^2$ .

The cadence time is defined as the mean time required to survey  $\Omega$ , but the survey may include a great deal of valuable

temporal sampling when the survey includes multiple exposures. For example, the PS1-3 $\pi$  survey is specifically designed to detect moving objects with pairs of exposures on a  $\sim 15$  minute interval. It is therefore not safe to conclude that  $t_{\text{cad}}$  listed in Table 2 is the shortest time interval for detection of motion or variability.

It is instructive to examine how the ATLAS proposal differs from HAT-South and Pan-STARRS 1. ATLAS is using a very similar approach to the HAT-South project, even to the extent of both using four Takahashi telescopes on common mounts, each feeding a  $4000 \times 4000$  camera. ATLAS gains factors in capability from  $\epsilon(\times 4)$ ,  $\omega(\times 3)$ ,  $\Omega(\times 1.5)$ , but loses in  $A(\times 0.7)$  for a net gain of about an order of magnitude. Pan-STARRS-1 and ATLAS have nearly the same product of  $A\Omega_0\epsilon$  (collect photons at the same rate), but, of course, Pan-STARRS-1 has about an order-of-magnitude-higher capability than ATLAS, because  $\omega$  is so much smaller.

It is not worthwhile to try to split hairs about which survey is the best or most capable; many of the parameters in Table 2 are rough enough that it is not possible to make an accurate comparison. Even more important, the table fails to clarify all the factors that make the various surveys especially well tuned for the science they are trying to do. However, ATLAS does occupy an important portion of design space. It is an order of magnitude faster than existing NEO surveys, it reaches much fainter magnitudes than the other subday cadence surveys, and it

<sup>15</sup> See <http://lsst.org>.

is unique in surveying the entire sky several times per night. While some of the other systems could move at constant capability to cover the entire sky nightly, they would not be able to do so at nearly the sensitivity of ATLAS.

ATLAS is complementary to general surveys such as Pan-STARRS, SkyMapper, and LSST. Like these, it covers most of the sky, but it offers a much faster cadence at the cost of less sensitivity, fewer colors, and less resolution. As described in the next section, there is a great deal of science to be found in this brighter, faster regime of discovery space, in addition to the primary mission of finding asteroids approaching the Earth.

## 5. SCIENCE WITH ATLAS

### 5.1. Asteroid Impacts

ATLAS is first and foremost a system to warn of incoming objects that might hit the Earth. ATLAS is not optimized to find objects at 1 AU and  $H \sim 20$ , many of which are known and will never strike the Earth. Other systems, notably Pan-STARRS and (eventually) LSST, have the leisure to find and catalog these objects better.

Fortunately, the interval between collisions of the Earth with an object of  $\sim 50$  m or larger is many centuries, the impact at Tunguska in 1908 notwithstanding. However, the cumulative frequency of Earth impacts as a function of the size of impactor has been estimated by Brown et al. (2002) as

$$N(> D) = 37 \text{ yr}^{-1} \left( \frac{D}{1 \text{ m}} \right)^{-2.7}, \quad (11)$$

so we can expect an impact of a 20–30 m asteroid once per century, a nearly megaton-class explosion. Although most of the incident energy will be dissipated high in the atmosphere, we have already discussed the evidence that it could cause significant damage on the ground as well.

We have developed a detailed ATLAS simulator that integrates the orbits of NEOs or impactors from Veres et al. (2009): either 10,000 impactors chosen to strike the Earth randomly in location and time over the next 100 yr or the full population of 270,000 NEOs. It is important to note that Earth impactors have a different orbit distribution from NEOs or even PHOs—the impactor’s orbit distribution is shifted to smaller semimajor axis, eccentricity, and inclination.<sup>16</sup> This is what makes ATLAS so effective at identifying *impactors* as opposed to generic NEOs. If an asteroid can hit the Earth, its orbit must intersect the Earth’s orbit, and ATLAS’s small search volume and fast cadence are ideal for finding them.

<sup>16</sup> An NEO is defined as an object with a perihelion less than 1.3 AU and an aphelion greater than 0.983 AU; a PHO is an object with  $H < 22$  (diameter  $\sim 140$  m) whose orbit passes within 0.05 AU of the Earth’s orbit; and an impactor is an object that actually strikes the Earth within 100 yr.

The simulator uses ATLAS’s view of each night’s sky, schedules the observing time; examines each asteroid for visibility according to its apparent magnitude and the observation’s extinction, trailing losses, and weather; and decides that an asteroid has been found when it has been observed eight times in four tracklets or else has an accurate parallax.

ATLAS can detect more than half of the impactors that are larger than 50 m and almost two-thirds of the 140 m impactors, as illustrated in Figure 3. The asteroids that ATLAS misses slip in from the direction of the Sun and South Pole or during periods of bad weather. (An ATLAS copy in the southern hemisphere or in a different weather pattern would raise the detection fraction.) Figure 4 illustrates the distribution of warning times provided by ATLAS. Objects of 140 m diameter are typically detected 20 days before impact, while 50 m diameter objects are detected with a week’s notice, when they are  $\sim 15$  times the distance to the moon.

Simultaneous images from the two sites provide a  $3\sigma$  parallax when the object is closer than 0.1 AU, about two weeks before impact. The parallax is crucial for identification of an approaching asteroid in a single night and important for vetoing confusion with space junk.

Looking at the full NEO and PHO populations, the right panel of Figure 4 shows the rate at which asteroids are found by ATLAS. ATLAS will (re)discover 50% of all 1000 m NEOs and PHOs within 1 yr, 70% in 3 yr, and 90% in 10 yr. The net rate of detection of 140 m asteroids or larger should be more than 400 NEOs and 100 PHOs per year. ATLAS can find about 15% of all 140 m PHOs within 3 yr and 30% within 10 yr, which is slightly less than Veres et al. (2009) found for the Pan-STARRS 1 mission.

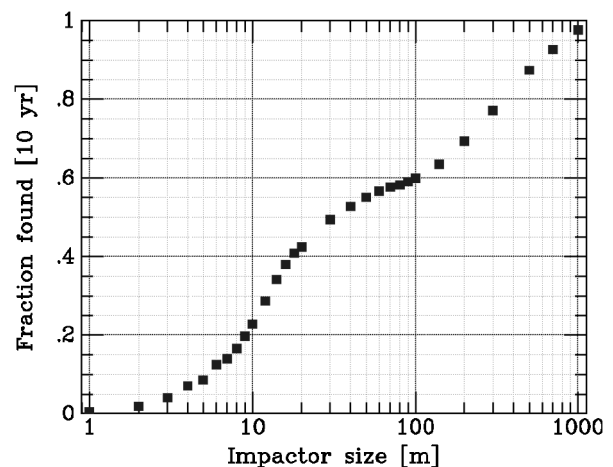


FIG. 3.—Fraction of impactors that ATLAS detects before collision, as a function of asteroid size for a survey of 10 yr duration. The kink at  $\sim 20$  m occurs when a significant fraction has warning time greater than one day, and the kink at  $\sim 140$  m is caused by an increasing fraction of greater than one orbit warning time. See the online edition of the *PASP* for color version of this figure.

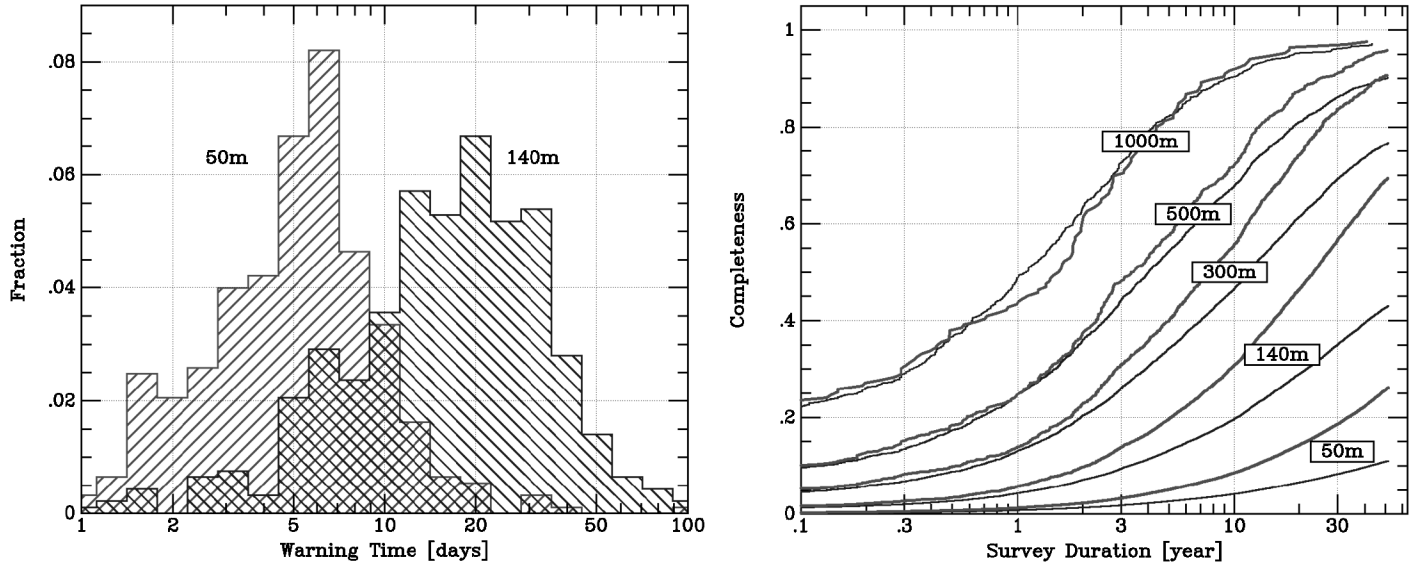


FIG. 4.—*Left:* Distribution of warning times provided by ATLAS for impactors of 140 m and 50 m diameter that it detects. The typical 140 m impactor will be found three weeks before arrival; the typical 50 m impactor will be found one week before collision. Depending on survey duration, there is also a growing number of warning times longer than a year (not illustrated here). *Right:* ATLAS’s completeness for detection of NEOs (thin lines) and PHOs (thick lines) of various sizes as a function of survey duration. See the online edition of the *PASP* for color version of this figure.

ATLAS is not a direct competitor for the much more capable surveys such as Pan-STARRS 4 or LSST. However, for the crucial days and weeks that an impactor is on final approach, ATLAS is far more effective than any existing NEO survey, Pan-STARRS, or LSST. The coverage and cadence that ATLAS provides give us a high probability of seeing an incoming asteroid, and ATLAS’s sensitivity is enough to spot it while it is still reasonably distant.

When ATLAS detects a nearby object it will automatically provide the measurements to the Minor Planet Center for posting on their Web-based NEO Confirmation Page. At that time, in a manner similar to the rapid follow-up of the first preimpact identification of meteoroid 2008 TC<sub>3</sub> (Jenniskens et al. 2009), we expect other amateur and professional observers to obtain additional observations. The case of 2008 TC<sub>3</sub> demonstrates the amazing accuracy that can be achieved: JPL’s predictions were accurate to  $\sim 20$  s and  $\sim 100$  km within hours of discovery, and the eventual prediction was accurate to  $\sim 1.5$  s and  $\sim 1$  km.

## 5.2. Asteroid Science

ATLAS will monitor a large number of asteroids in the Main Belt as well as asteroids and comets elsewhere in the solar system. The rapid time cadence of ATLAS is particularly well suited to providing light curves and simultaneous colors for many asteroids that can then be analyzed to infer asteroid shape and tumbling motion. ATLAS should achieve photometry in two colors with 0.01 mag accuracy at  $V \sim 16$ , 0.02 mag accuracy at  $V \sim 17$ , and 0.04 mag accuracy at  $V \sim 18$ . The AstDyS

Web site<sup>17</sup> () lists 973 numbered asteroids with  $V < 16$ , 3149 with  $V < 17$ , and 10,078 with  $V < 18$  at this moment in time (2010 October 10) in the three-eighths sky between R.A. of 18<sup>h</sup> to 6<sup>h</sup> and decl. of  $-30^\circ$  to  $+90^\circ$ . Most are considerably off of opposition right now, and so they have been (or will be) brighter during the 4–5 months it takes to sweep by. Therefore, ATLAS should provide twice-nightly two-color light curves of  $\sim 4$  month duration for at least 2000 asteroids with an accuracy of 0.01 mag per point, 6000 asteroids with an accuracy of 0.02 mag, and 20,000 asteroids with an accuracy of 0.04 mag.

It has been estimated by R. Jedicke (2010, private communication) that there is a collision each day that disrupts a 10 m asteroid in the Main Belt. If the dust cloud from the collision grows to 1000 m before becoming optically thin, the collision should be detectable by ATLAS. The recent asteroid collision event P/2010 A2 discovered by LINEAR achieved  $m \sim 19$  and would be detectable by ATLAS.

An object in the outer solar system must have  $H < 4$  to be detectable by ATLAS, so ATLAS is unlikely to add many new discoveries to the bodies already known or that will be discovered by Pan-STARRS 1. The value from ATLAS is completeness and ongoing monitoring of three-fourths of the sky. If an object has slipped between the cracks of other surveys, happens to brighten (e.g., tumbling), or is rapidly approaching (e.g., new comets), ATLAS may be the first to discover it. The current IAU definition of a dwarf planet is a body with  $H < 1$ . With full illumination, at 60 AU distance (approximately the outer edge

<sup>17</sup> See <http://hamilton.dm.unipi.it/astdys>.

of the Kuiper Belt), such a body would have a  $V$  magnitude of 18.8 and would therefore be easily detectable by ATLAS. ATLAS should therefore detect virtually all dwarf planets in the solar system within one year and should be particularly useful for searching well out of the ecliptic, where such bodies might have scattered.

### 5.3. Supernovae

Supernovae Type Ia (SNe Ia) have proven utility as measures of the cosmological expansion of the universe and could continue with even more subtle questions, such as whether the accelerated expansion is consistent with a cosmological constant. Since we do not very well understand the environment, initial conditions, trigger mechanism, and explosion process of SNe Ia, these extremely delicate measurements are vulnerable to systematic errors.

A Type Ia supernova at  $z = 0.1$  peaks at  $V = 18.9$ . The ATLAS sensitivity at  $S/N = 10$  is  $19.5 \text{ day}^{-1}$ ; assuming 70% clear weather, the ATLAS sensitivity for four nights is  $V = 20.1$  for  $S/N = 10$ . According to Mannucci et al. (2007), there are approximately 9000 SNe Ia yearly that are closer than  $z = 0.1$  (32,000 at  $z < 0.15$ ). Since the area that ATLAS surveys each night is half of the entire sky (neglecting obscuration by the Galactic plane), we can expect that ATLAS will find and follow 4500 SNe Ia per year at  $z < 0.1$  and  $S/N > 30$  and follow 16,000 SNe Ia per year at  $z < 0.15$  with  $S/N > 14$ , with a 4 day sampling of the light curve. Perhaps more interesting from the standpoint of investigating systematics, ATLAS should find approximately 300 SNe Ia per year that peak at  $V < 17$  and  $\sim 30$  per year that peak at  $V < 15$ . This is nearly an order of magnitude greater than the discovery rate of bright SNe Ia over the past decade and has the advantage of being completely unbiased. By contrast, the Katzman Automatic Imaging Telescope (Li et al. 2003) finds approximately 75 supernovae per year by patrolling nearby galaxies.

The huge number of SNe Ia discovered by ATLAS, as well as the completeness of examining the entire sky, will empower us to ask questions regarding the characterization of explosion as a function of host galaxy properties, details of the very early phases of the explosion, and identification of outlier events that can be flagged for spectroscopy or more detailed photometry. We can also expect to see a large number of SNe Ia in interesting environments such as rich clusters or tidal streams of interacting galaxies.

Core-collapse supernovae (CCSNe) are particularly interesting when they result in a huge collimated explosion, creating a gamma-ray burst. These are thought to occur in low-metallicity environments from WR stars that have a high core angular momentum at the time of collapse. Young et al. (2008) estimated that there are 20 CCSNe per year in galaxies with  $12 + \log(\text{O}/\text{H}) < 8.2$  and  $z < 0.04$ . ATLAS's nightly  $10\sigma$  sensitivity of  $V = 19.5$  translates to  $V = 18.5$  at  $25\sigma$ . In 10 days' time (seven clear nights), ATLAS achieves  $V = 19.6$  at  $25\sigma$ . CCSNe

peak at  $M \sim -16.8$  (II-P),  $M \sim -18.3$  (Ib/c), and  $M \sim -19.6$  (II-L), and the distance modulus at  $z = 0.04$  is  $(m - M) = 36.2$ , so ATLAS should be able to detect all of these outbursts at  $25\sigma$ , extinction permitting. Since ATLAS is surveying half of the sky, the expected number is 10 CCSNe per year in such low-metallicity galaxies.

### 5.4. Gravity Waves

Although Laser Interferometer Gravitational-Wave Observatory (LIGO) has yet to detect a gravity wave (GW) event, it is virtually certain that gravity waves exist and highly likely that Advanced LIGO will detect GW events. The most common detections will be coalescing compact objects whose changing quadrupole moment makes a vigorous, detectable chirp in gravity waves. Abadie et al. (2010) estimated the rates of events and sensitivities and suggest that the most likely events will be neutron-star/neutron-star (NS-NS) coalescence within  $\sim 445$  Mpc.

While, in principle, a coalescence of naked compact objects could give rise to a minimal electromagnetic signature, it seems quite possible that the release of more than  $10^{53}$  ergs of energy might be accompanied by  $10^{48}$  ergs in the optical, as argued by Stubbs (2008). Such an explosion corresponds to a luminosity with absolute magnitude of  $M \sim -18$  for a duration of 2 days. We do not try to advocate any particular mechanism, but only make the point that if even a part in  $10^{-5}$  of the energy release appears in the optical, it will be a substantial luminosity for a substantial duration.

Abadie et al. (2010) estimated that one NS-NS coalescence occurs every million years in every  $\text{Mpc}^3$ , and they therefore expected to see some 40 events per year, applying a factor of 2.26 to the horizon distance of 445 Mpc to account for sky location and orientation. The distance modulus of 445 Mpc is 38.2, so an explosion of  $M = -18$  would be just detectable by ATLAS, provided that it happens within the half-sky visible to ATLAS and endures long enough for ATLAS to sweep across it. The nearest object that Advanced LIGO would see in 1 yr would be a factor of  $40^{1/3}$  closer, 2.7 mag brighter, and easily seen by ATLAS.

The coalescence of compact objects creates a well-defined GW signal and an extremely ill-defined optical transient. On the other hand, CCSNe are common, and Ott (2009) reviewed their possible GW signatures and the ability of Advanced LIGO to detect them. Advanced LIGO may be able to detect a CCSN within 1 Mpc with  $S/N = \sim 6$ , but the rate of such supernovae within the Local Group is only one in  $\sim 20$  yr. There is about one CCSN each year within  $\sim 5$  Mpc, and the rate grows rapidly at distances beyond  $\sim 8$  Mpc that start to reach into the Virgo cluster.

CCSNe closer than the Virgo cluster will be much brighter than the ATLAS magnitude limit of 20, and therefore ATLAS will detect the half of them that are in the visible sky at the time of explosion. We have a decent chance over a year or two of matching an Advanced LIGO event at  $3\sigma$  with a CCSN seen

by ATLAS, but there is no question that ATLAS will provide times and locations for many events for which Advanced LIGO may have a  $\sim 1\sigma$  detection. The time between collapse and emergence of the light flash is short enough that it should be possible to correlate CCSNe events with low-S/N GW events and thereby learn about the mechanism by which CCSNe events create gravity waves.

### 5.5. Novae, Outbursts, and Variable Stars

Novae range in absolute magnitude from  $M_V = -9$  to  $M_V = -7$ , declining by 3 mag in a week to several months, and the number per galaxy is estimated to be approximately 40 per year. ATLAS's 4 day  $10\sigma$  sensitivity of  $V = 20.3$  gives us the ability to see novae to distance moduli of  $(m - M) \sim 28$ ; i.e., we will certainly see all the novae in the Milky Way and M31 within ATLAS's half-sky, and most of the novae in nearby galaxies such as M81 and M101, but we will not see novae in the galaxies in the Virgo cluster.

Luminous blue variable stars flare at  $M_V \sim -9$  to  $M_V \sim -13$ , so again, ATLAS can find and monitor many of them on a daily basis to distances as great as the Virgo cluster.

Mira variables peak at  $M_V \sim -1.5$  with periods of the order of 100 days, and FU Orionis outbursts peak in the range of  $M_V \sim -1$ , rising over a year and then declining over decades. ATLAS can monitor these all throughout the Galaxy, although M31 is too distant. A southern ATLAS would encompass the Magellanic Clouds, at distance modulus 18, and so it is sensitive at  $10\sigma$  to  $M_V = +2$  and brighter.

There are approximately 2000 cataclysmic variables known in the neighborhood of the Sun. ATLAS is unique in being able to keep an eye on all of them, with two samples each day spread by an hour or two. This will provide excellent sampling of their periods (typically about an hour), as well as providing an alert within a day of an interesting outburst. Within 1 kpc ATLAS has a  $10\sigma$  sensitivity at  $M_V = +9$  per visit.

Of course, ATLAS will also watch the lesser beasts of the variable zoo in the sky. At 20 kpc ATLAS's sensitivity at  $10\sigma \text{ day}^{-1}$  is  $M = +3$ , so all instability strip stars such as RR Lyrae and Cepheids will have daily observations at high S/N. ATLAS will provide the first opportunity to catalog all the eclipsing and variable binary stars in the sky to  $M = +3$  or fainter. ATLAS's blue filter is deliberately truncated short of  $H\alpha$ , so ATLAS has special sensitivity to  $H\alpha$  flares—variability that is extremely red is likely to arise from  $H\alpha$ .

### 5.6. Active Galactic Nuclei

Croom et al. (2004) analyzed the active galactic nuclei (AGNs) luminosity function in the SDSS DR5, from which we calculate that there are approximately a half-million AGNs in the sky brighter than  $V = 19.6$ . At that level ATLAS can monitor half of them, more than 100,000, at  $25\sigma$  for a 10 day cadence or  $10\sigma$  for a daily cadence. AGNs have a com-

plex structure function of variability ranging from general flickering of the accretion process to flares from tidal events to the spectacular luminosities of blazars and their instabilities. ATLAS's sensitivity, solid angle, and cadence have an excellent overlap with the densities of AGNs and their various sources of variation. Well-sampled light curves with timescales ranging from days to years are key to studying AGN variability.

At  $V = 20$  there are 1800 galaxies per square degree, so ATLAS will maintain a daily watch on approximately 40 million galaxies, sensitive to events whose luminosity is comparable with that of the galaxy on a 1 day timescale or longer. For example, a star is occasionally disrupted by accretion onto a black hole at the center of a galaxy, producing a flare of predictable color and duration. Gezari et al. (2009) predicted a volume rate of  $2.3 \times 10^{-6} \text{ yr}^{-1} \text{ Mpc}^{-3}$  and calculated that a survey with  $g < 19$  would detect events out to 200 Mpc, corresponding to a detection rate of 20 events per year by ATLAS.

### 5.7. Lensing

Even at the north Galactic pole there are about 2000 stars per square degree brighter than the 1 day limiting magnitude of  $V = 20$ . Over the entire  $20,000 \text{ deg}^2$  being surveyed each night by ATLAS there are about a half-billion stars far enough off of the Galactic plane that there is manageable confusion in ATLAS's  $4.4''$  pixels.

Han (2008) estimated the rate of near-field microlensing from all-sky surveys and found that at  $V = 18$  we can expect to see 23 events per year, where an event is defined as an increase of source flux by more than 0.32 mag. The number scales inversely with the star's flux, so at  $V = 19$  there should be 58 lensing events over the sky per year. At  $V = 18$  the lens-source proper motion can exceed  $40 \text{ mas yr}^{-1}$ , so we could hope to disentangle their light after a few years by imaging from space- or ground-based adaptive optics. The event timescales at the fainter limits are about 20 days.

ATLAS will survey half of the entire sky at  $S/N = 10 \text{ night}^{-1}$  at  $V = 19.5$ , so a  $V = 18$  star will be captured with 0.025 mag uncertainty each night and a  $V = 19$  star will have 0.06 mag error each night. A 0.3 mag lensing event will therefore be seen at  $10\sigma$  at  $V = 18$  and at  $5\sigma$  at  $V = 19$ . Over 20 nights, even allowing for weather, ATLAS ought to capture most events to  $V < 19$ , and the two filters will permit some level of testing of achromaticity. We therefore estimate that ATLAS should see approximately 30 microlensing events in the near field each year, and 10 should have high S/N and time coverage.

There is a surprisingly large cross section for strong gravitational lensing by galaxy centers. We integrated the galaxy velocity dispersion function of Sheth et al. (2003), using both the densities listed for early-type galaxies and late-type galaxy bulges, assuming that each galaxy has an isothermal core that is capable of lensing. Over the entire sky, the cross section for a lensing magnification of 3 or greater is  $0.37 \text{ deg}^2$  for sources at

a redshift of  $z = 0.5$ ,  $1.75 \text{ deg}^2$  for sources at a redshift of  $z = 1.0$ , etc., scaling as  $(\mu - 1)^{-2}$ , where  $\mu$  is the lensing magnification, and as  $z^3$  in the Euclidean limit. Divided by the  $41,250 \text{ deg}^2$  of the sky, this cross section provides a magnification probability.

The number of lensed SNe Ia that ATLAS will see, even aided by magnification, will barely yield one event per year. Integrating the density of SNe Ia from Mannucci et al. (2007) against the lensing cross section, we expect to see one lensing event per year peaking at a (magnified) magnitude of 20.6. Of course, this will be extremely hard to distinguish from the hordes of SNe Ia close to galaxy centers.

However, the number of magnified AGNs that ATLAS will detect is quite large. Integrating the luminosity function of Croom et al. (2004) against this cross section gives more than 40 AGNs in the sky with a magnification of 3 or larger at a magnitude of 19.6 or brighter ( $25\sigma$  at 10 days and  $10\sigma$  at 1 day). Among these, there are  $\sim 7$  at magnification 10 or greater. The lensing cross section grows rapidly with redshift, of course, so this is an interesting probe of AGN density, AGN variability as a function of redshift, and galaxy core structure as a function of redshift. At high magnifications the microlensing by stars within the lensing galaxy can cause substantial flickering as well.

### 5.8. The Static Sky

ATLAS has only modest sensitivity on a per-unit telescope basis, and it undersamples a point-spread function that will average about  $2.5''$  from atmosphere and optics, but the S/N grows, as each piece of the sky gets approximately 350 visits per year (3.1 mag). Figure 5 compares how an  $0.01 \text{ deg}^2$  piece of sky appears in the digital POSS sky survey, the SDSS sky survey, and ATLAS.

ATLAS goes substantially deeper than POSS after a week of observation, even allowing for weather. The SDSS PSF is considerably better than ATLAS can ever achieve, but Figure 6 illustrates how the color co-added sky would look after a year of ATLAS observation (with allowances for weather).

After a year's operation ATLAS is significantly deeper than SDSS (and covers three-fourths of the sky), although the coarse sampling eventually runs into source confusion. However, the density of transient and variable objects is far lower than the density of static objects, so ATLAS should stay above the confusion limit for detection and characterization of the variable parts of their light curves, with S/N proportional to the square root of the timescale. For example, ATLAS can achieve  $m \sim 23$  sensitivity for slow events such as AGN variability or long-period variable stars.

### 5.9. Space Junk

There is a growing amount of space junk in low Earth orbit (LEO) and geosynchronous Earth orbit (GEO). This is of some

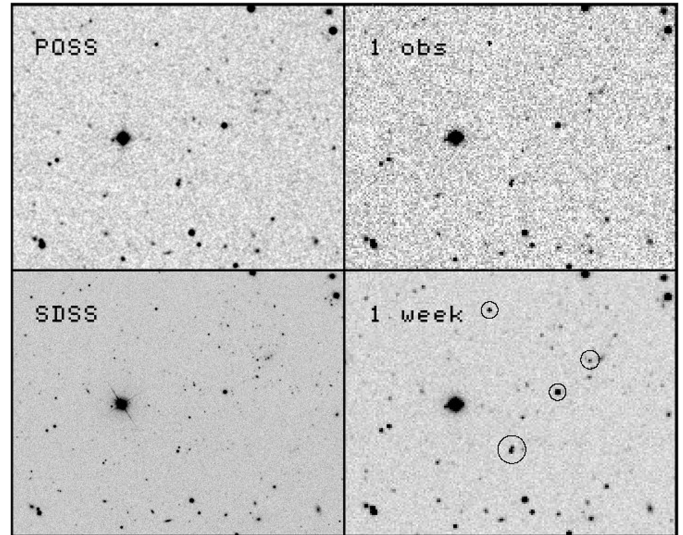


FIG. 5.—Upper left: Appearance of an  $0.1 \times 0.08 \text{ deg}$  portion of the sky in POSS  $R$  band. Lower left: View in the SDSS  $r$  band. Upper right: How it would appear in a single ATLAS red observation (two 30 s integrations). Lower right: After a week of observation (five clear nights). The circled stars are  $m = 17$ ,  $m = 18.5$ ,  $m = 19.4$  ( $5\sigma$ ), and a pair at  $m = 18.2$  and  $19.2$  separated by  $4.4''$ .

concern for satellites and space travel, as evidenced by the recent destruction of an iridium satellite by collision with a tumbling booster. To sky surveys looking for transients and moving objects, space junk is a significant background signal that masks the solar system objects in which we are interested.

A good rule of thumb for the detection of a streak across an image left by a moving object is that when each PSF-sized

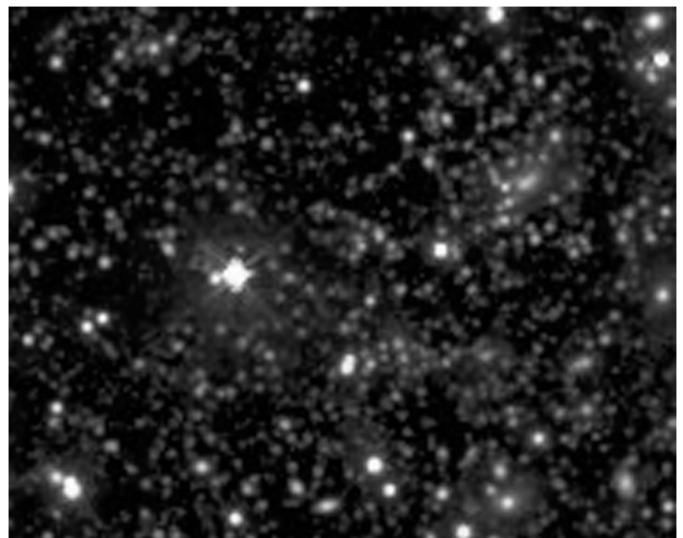


FIG. 6.—Image of the  $0.1 \times 0.08 \text{ deg}$  portion of the sky after a year of ATLAS observation illustrates the appearance of  $S/N = 10\sigma$  at  $V = 22.4$ . Although static objects are starting to blend together at this limit, variable objects are rare enough to stand out cleanly once the static sky is subtracted. See the online edition of the *PASP* for color version of this figure.

segment of the streak is  $1\sigma$  above background, it is easily visible to the eye and easily detectable. A magnitude fainter is harder, and two magnitudes fainter is just about the limit of what can be detected.

A LEO object at the 1000 km range moves at about  $0.4^\circ \text{ s}^{-1}$ . ATLAS has four views (two staggered by  $5^\circ$  at each site) and two sites, so many objects will have one or two endpoints caught by the system. A LEO object will spend 3 ms on a pixel, and therefore the  $1\sigma$  routine detection benchmark is 8.3 mag brighter than the  $5\sigma$  magnitude limit for a 30 s exposure: i.e., about  $m = 10.8$ . At  $m = 11.8$  the streak will be visible to the eye and should be possible to detect automatically, particularly given the confirmation from the two sites and the possible collection by the adjacent pointing.

This magnitude corresponds to a white, fully illuminated, Lambertian ball of size  $\sim 4$  cm or a piece of space junk of size  $\sim 15$  cm of albedo 0.1 and random illumination. There are estimated to be of the order of 10,000 objects in LEO of that size or greater.

A GEO object only moves at  $15'' \text{ s}^{-1}$ , spending 0.3 s on a pixel, so the  $1\sigma$  benchmark is 5 mag fainter than LEO: i.e.,  $m = 15.8$ . Automated detection should therefore be possible to  $m = 16.8$  ( $\sim 60$  cm) without much trouble. At the 40,000 km range, the tangential position accuracy should be approximately 100 m, and the range accuracy should be about 50 km for the single observation. Since ATLAS sweeps the visible sky twice each night, GEO objects will be captured on two occasions, permitting a good estimate of orbit.

## 6. WORLD-WIDE INTERNET SURVEY TELESCOPE

Apart from its value as a survey for hazardous asteroids, ATLAS also serves to define a unit survey telescope and software that can be replicated many times in order to improve on the networked performance. ATLAS could therefore be a template for a World-wide Internet Survey Telescope (WIST) that has as many unit observatories as there are parties who would like to participate, since it is sized to fit within the budget of any college or university.

The ATLAS proposal to NASA is carefully optimized to take advantage of the existing  $\sim 1.3$  million worth of detectors; tries to avoid as much hardware risk as possible by using commercial components; and plans for software research and development to be the most costly, difficult, and critical aspect of the project. However, given time and resources for hardware research and development, it is possible to develop a successor that would have considerably greater capability per unit cost than the present ATLAS implementation.

For example, a remarkable set of designs by M. Akermann, J. T. McGraw, and P. C. Zimmer (2010, private communication) include an 0.5 m aperture Hamilton astrograph with 1 m focal length and  $7^\circ$  field of view that achieves 50% encircled energy at 1.5  $\mu\text{m}$  radius: i.e., half-energy within a diameter of  $0.6''$ . The optimal unit camera could have 5–9  $\mu\text{m}$  pixels (0.5–0.2 Gpixel

total) for a 1–1.8'' sampling over a field of view of  $\sim 40 \text{ deg}^2$ . We note the growing availability of large-format detectors, such as the STA-1600 CCD<sup>18</sup> that has  $10,000 \times 10,000$  9  $\mu\text{m}$  pixels and can read out at 1 frame per second, Canon's recent announcement of an APS-H format ( $29 \times 20$  mm), 120 Mpixel complementary metal oxide semiconductor (CMOS) sensor as well as a monolithic  $202 \times 205$  mm, high-sensitivity sensor, and advances in back-illuminated CMOS detectors by Cypress, Sony, and others. It is conceivable that improvements in capability per unit cost of a factor of 3 or more might emerge.

We have therefore tried to think of ATLAS as the start of a franchise that defines what a hardware and software unit should be: basically, a high-performance telescope and detector system in a robotic observatory, with common reduction and analysis pipeline and common protocols for communications. An essential component is bandwidth management—the ATLAS system has enough local processing to handle the  $\sim 100$  GB night<sup>-1</sup> of raw data and depends on extra-observatory bandwidth, primarily for trading object catalogs that will have orders-of-magnitude-less information.

The Las Cumbres Observatory Global Telescope (LCOGT; Brown et al. 2002) consists of a widely distributed set of many telescopes that are intended for full-time synoptic coverage of interesting events such as planet occultations or microlensing passages. WIST differs by being dedicated to all-sky, nightly survey, and discovery. WIST and LCOGT are therefore complementary in their approaches and scientific goals, although both are striving to make the greatest possible use of the silicon revolution and the Internet.

Because we want to achieve the highest possible hardware and software performance, and also because we cannot cope with the difficulties inherent in a National Virtual Observatory that tries to accept information of varying quality and provenance, the WIST franchise would insist on a very high degree of standardization. This does not mean that a college with poor seeing or bright skies cannot participate. WIST is intended to be tolerant of poor seeing, and the standardization allows us to replace metrics that permit optimal combination of information from all sites.

As the number of observatories grows it would become possible to schedule dynamically according to weather and to allocate observations by filter or time to different places. Sites with very bright sky backgrounds might be assigned very short exposure times for a more rapid cadence on bright objects, for example. Obviously, the search for approaching impactors can be significantly improved by WIST, by virtue of closing the southern blind spot, squeezing down the solar blind spot, immunity to weather, and deeper imagery.

Since we intend that the cost of WIST be borne by the participants, we expect that all results would be made public

<sup>18</sup> See <http://www.sta-inc.net>.

immediately. This will encourage participants to define and carry out projects promptly, and we hope it will encourage collaborations. The fact that WIST puts the smallest colleges on the same footing with the most prestigious research universities will serve to foster innovation and reduce the dependence of research achievement on availability of resources.

## 7. CONCLUSION

In this article we have argued that the congressional mandate to NASA to mitigate the hazard from asteroid impact on Earth can be parsed temporally as well as by impactor size. To some degree the risk can never be reduced to zero because orbits are continually perturbed, but we believe that the most important *time interval* for discovery of small impactors is just before impact, and we have demonstrated that it is relatively easy and cost-effective to patrol that portion of hazard space.

In order to understand the real capability of survey systems, we examined the meaning of etendue and survey capability and derived equations that quantify survey capability both in terms of hardware specifications of aperture, solid angle, efficiency, and image quality and in terms of actual performance. In support of this we also derived an equation that quantifies the image performance in terms of an effective noise footprint, which is valid even in the regime of pixels that undersample the PSF.

We advanced a description of a new survey instrument, called the Asteroid Terrestrial-impact Last Alert System. ATLAS surveys 20,000 deg<sup>2</sup> twice per night to magnitude 20, with the sensitivity determined by the practical need for three weeks' warning of a 100 Mton impact and with the solid angle determined by the practical need for immediate warning of a 1 Mton impact. The components for an ATLAS system are mostly available commercially, the cost is low, and the construction time is short.

We compared ATLAS with the other prominent sky surveys in operation or being planned and found that ATLAS has interesting complementarities to the other surveys that make it particularly potent for early warning of impacts by hazardous objects: it surveys essentially the entire sky at a rapid cadence, so the probability of any object slipping through is reasonably

low and its sensitivity is high enough to provide a useful warning. No other survey is as effective for this particular job.

Of course, the ATLAS imagery will also open an interesting window on the entire transient universe. Some of the additional science products that ATLAS will produce include:

1. Hundreds of light-curve points for thousands of asteroids that provide estimates of shape and spin.
2. Detection of all dwarf planets in the solar system.
3. Twice-per-night monitoring of ~2000 cataclysmic variables.
4. Detection of ~30 near-field microlensing events per year.
5. Twice-per-night light curves of most variable stars in the Galaxy.
6. Novae and luminous blue variable outbursts in most nearby galaxies.
7. Detailed and prompt information on electromagnetic counterparts to gravity wave events.
8. Detection of ~10 core-collapse SNe in low-metallicity galaxies per year.
9. Light curves of ~4000 SNe Ia per year with  $z < 0.1$ , ~300 with  $V < 17$ .
10. Variability of ~100,000 AGNs.

We ended with consideration of a future World-wide Internet Survey Telescope (WIST), comprised of a confederation of many basic observatory units. The intent is to franchise the hardware and software design, but at a cost point that makes an observatory unit affordable by essentially any college or university. This standardization is necessary to allow the full system to be scheduled and for the results of the imagery to be optimally combined, but leads to a system that is virtually unbounded in its ability to explore the time and sensitivity domains of the transient universe. Support for this work was provided by National Science Foundation grant AST-1009749.

We acknowledge useful discussions with Christopher Stubbs, Robert Jedicke, Armin Rest, and John Blakeslee. We are grateful for the remarkable design work of Mark Ackermann, John McGraw, and Peter Zimmer. This article benefited from discussions at the Aspen Center for Physics.

## REFERENCES

- Abadie, J., et al. 2010, *Classical Quantum Gravity*, 27, 17, 173001
- Asphaug, E. 2009, *Annu. Rev. Earth Planet. Sci.*, 37, 413
- Bakos, G., et al. 2009, in *IAU Symp. 253, Transiting Planets*, ed. F. Pont, D. Sasselov, & M. Holman (Cambridge: Cambridge Univ. Press), 354
- Boslough, M. B. E., & Crawford, D. A. 2008, *Impact Engineering*, 35, 1441
- Brown, M. E., Bouchez, A. H., & Griffith, C. A. 2002, *Nature*, 420, 795
- Burgett, W., & Kaiser, N. 2009, *Proc. Adv. Maui Optical and Space Surveillance Technologies Conf.*, ed. S. Ryan (Maui: Maui Economic Development Board), E39
- Croom, S. M., Smith, R. J., Boyle, B. J., Shanks, T., Miller, L., Outram, P. J., & Loaring, N. S. 2004, *MNRAS*, 349, 1397
- Gezari, S., et al. 2009, *ApJ*, 698, 1367
- Han, C. 2008, *ApJ*, 681, 806
- Ivezic, Z., Tyson, J. A., Allsman, R., Andrew, J., & Angel, R., for the LSST Collaboration 2008, preprint (arXiv:0805.2366)
- Jenniskens, P., et al. 2009, *Nature*, 458, 485
- Keller, S. C., et al. 2007, *PASA*, 24, 1
- Larson, S., Beshore, E., Hill, R., Christensen, E., McLean, D., Kolar, S., McNaught, R., & Garradd, G. 2003, *BAAS*, 35, 982
- Larsen, J., Roe, E., Albert, E., Descour, A., McMillan, R., Gleason, A., Jedicke, R., Block, M., et al. 2007, *AJ*, 133, 1247

- Law, N. M., et al. 2009, *PASP*, 121, 1395
- Li, W., Filippenko, A. V., Chornock, R., & Jha, S. 2003, *PASP*, 115, 844
- Malek, K., Batsch T., Cwiok M., Dominik W., Kasprowicz G., Majcher A., Majczyna A., Mankiewicz L., et al. 2009, *Proc. SPIE*, Vol. 7502, 75020D
- Mannucci, F., Della Valle, M., & Panagia, N. 2007, *MNRAS*, 377, 1229
- McMillan, R. S., & Spacewatch Team 2006, in *IAU Symp. 236, Near Earth Objects, Our Celestial Neighbors, Opportunity and Risk*, ed. A. Milani, G. B. Valsecchi, & D. Vokrouhlicky (Cambridge: Cambridge Univ. Press), 2, 329
- Melosh, H. J., & Collins, G. S. 2005, *Nature*, 434, 157
- Morbidelli, A., et al. 2002, *Icarus*, 158, 329
- NASA, Near-Earth Object Survey and Deflection Analysis of Alternatives, 2007 (Washington: NASA), [http://www.nasa.gov/pdf/171331main\\_NEO\\_report\\_march07.pdf](http://www.nasa.gov/pdf/171331main_NEO_report_march07.pdf)
- National Research Council, 2010, *Defending Planet Earth: Near-Earth Object Surveys and Hazard Mitigation Strategies*, (Washington: National Academies Press)
- Ott, C. D. 2009, *Classical Quantum Gravity*, 26, 6, 063001
- Pollacco, D. L., et al. 2006, *PASP*, 118, 1407
- Sheth, R. K., et al. 2003, *ApJ*, 594, 225
- Schechter, P., Mateo, M., & Saha, A. 1993, *PASP*, 105, 1342
- Stokes, G. H., Evans, J. B., Vighh, H. E. M., Shelly, F. C., & Pearce, E. C. 2000, *Icarus*, 148, 21
- Stubbs, C. W. 2008, *Classical Quantum Gravity*, 25, 184033
- Trujillo, I., Aguerri, J. A. L., Cepa, J., & Gutiérrez, C. M. 2001, *MNRAS*, 328, 977
- Veres, P., Jedicke, R., Wainscoat, R., Granvik, M., Chesley, S., Abe, S., Denneau, L., & Grav, T. 2009, *Icarus*, 203, 472
- Vestrand, W. T., Albright, K., Casperson, D., Fenimore, E., Ho, C., Priedhorsky, W., White, R., & Wren, J. 2003, in *AIP Conf. Proc. 162, Gamma-Ray Burst and Afterglow Astronomy 2001: A Workshop Celebrating the First Year of the HETE Mission*, (New York: AIP), 550
- Young, D. R., Smartt, S. J., Mattila, S., Tanvir, N. R., Bersier, D., Chambers, K. C., Kaiser, N., & Tonry, J. L. 2008, *A&A*, 489, 359